RAFT-Mediated Polymerization

Deutsche Ausgabe: DOI: 10.1002/ange.201511159
Internationale Ausgabe: DOI: 10.1002/anie.201511159

The Effect of Hydrophile Topology in RAFT-Mediated Polymerization-Induced Self-Assembly

Jennifer Lesage de la Haye, Xuewei Zhang, Isabelle Chaduc, Fabrice Brunel, Muriel Lansalot, and Franck D'Agosto**

Abstract: *Polymerization-induced self-assembly (PISA) was employed to compare the self-assembly of different amphiphilic block copolymers. They were obtained by emulsion polymerization of styrene in water using hydrophilic poly(N-acryloylmorpholine) (PNAM)-based macromolecular RAFT agents with different structures. An average of three poly (ethylene glycol acrylate) (PEGA) units were introduced either at the beginning, statistically, or at the end of a PNAM backbone, resulting in formation of nanometric vesicles and spheres from the two former macroRAFT architectures, and large vesicles from the latter. Compared to the spheres obtained with a pure PNAM macroRAFT agent, composite macroRAFT architectures promoted a dramatic morphological change. The change was induced by the presence of PEGA hydrophilic side-chains close to the hydrophobic polystyrene segment.*

The self-assembly of block copolymers in solution has been the focus of many exciting studies owing to a corresponding broad range of potential applications.[1] This relies on the various morphologies that can be obtained by selecting a suitable solvent of one of the two blocks.[2] In the particular case of amphiphilic block copolymers, water can be used to generate spherical or cylindrical (worms/fibers) micelles, or vesicles from a diluted solution of the preformed amphiphilic block copolymer by the so-called co-solvent method. This property, which was largely studied by Eisenberg and coworkers[3] since the 1990s, is analogous with the behavior of molecular amphiphiles.[4] Self-assembly of molecular amphiphiles has been thoroughly rationalized by Israelachvili,[5] who showed that the resulting nanostructures could be predicted by the packing parameter (*P*) defined by the ratio of the volume of hydrophobic chains (v) divided by the product of the optimal area of the head group (a_0) and the length of the hydrophobic tail (l_c). Although easily determined for molecular surfactants, these parameters cannot be applied to block copolymers, and the hydrophobic/hydrophilic balance is generally considered instead. In this case, *P* depends on the relative volume fractions of the hydrophilic and hydrophobic blocks, and the interfacial energy associated with the di-block junction. Varying the relative volume fractions of each block (by altering their molar masses) usually dictates the final morphology. This is the result of the inherent molecular curvature and its influence on the packing of copolymer chains.[4b]

Among the large number of studies dedicated to self-assembly of amphiphilic block copolymers, only a few focus on the effect of hydrophile topology on the final morphologies. In parallel with the first report by Eisenberg,[3a] van Hest et al. showed that aggregation in water of preformed amphiphilic block copolymers based on a hydrophobic polystyrene block and hydrophilic polypropyleneimine dendrons was governed by generation of the latter.[6] The finding enabled consistent prediction of structures based on the packing parameter. Synthesizing DNA-brush copolymer amphiphiles, Chien et al. reported that micelle morphologies could be governed by selective cleavage in the DNA shell,[7] resulting in manipulation of the magnitude of steric and electrostatic repulsions within the shell, and thus of the packing parameter. Very recently, Martinez et al. synthesized polystyrene-*b*-polyisoprene (PS-*b*-PI) block copolymers using anionic polymerization.[8] Poly(ethylene glycol) side-chains were grafted onto the polyisoprene segment. The morphologies formed by aqueous self-assembly of the resulting amphiphilic block copolymers were dependent upon the brush density. Densely grafted polymers only formed spherical micelles, whereas sparsely grafted brushes formed higher-order structures, including cylindrical micelles and vesicles. Lovett et al. showed that ionization of a single carboxylic acid group on the hydrophilic block of a preformed amphiphilic block copolymer (namely poly(glycerol monomethacrylate)-*b*-poly(2-hydroxypropyl methacrylate)), sufficiently increased the degree of hydration of the hydrophilic segment to induce a morphological transition from worms to spheres after dissolution of pre-formed worms and re-assembly.[9]

The recent application of controlled radical polymerization (CRP) techniques to dispersed media (in dispersion and emulsion polymerization for example)[10] has unlocked a powerful new approach for producing self-assembled nano-objects. This approach, known as polymerization-induced self-assembly (PISA), starts with a hydrophilic living polymer chain that is extended in water using hydrophobic monomers. Consequently, amphiphilic block copolymers self-assemble in tandem with growth of the hydrophobic block, resulting in the aforementioned morphologies. A morphological evolution from spheres to worms to vesicles can be observed during this type of PISA synthesis, which is driven by the increase of the packing parameter as the core-forming block grows. Com-

[*] Dr. J. Lesage de la Haye, Dr. X. Zhang, Dr. I. Chaduc, Dr. F. Brunel, Dr. M. Lansalot, Dr. F. D'Agosto
Université de Lyon, Univ Lyon 1, CPE Lyon, CNRS, UMR 5265, C2P2 (Chemistry, Catalysis, Polymers & Processes), Team LCPP Bat 308F
43 Bd du 11 Novembre 1918, 69616 Villeurbanne (France)
E-mail: muriel.lansalot@univ-lyon1.fr
franck.dagosto@univ-lyon1.fr

Supporting information for this article is available on the WWW under http://dx.doi.org/10.1002/anie.201511159.

pared to the co-solvent method, PISA offers an extremely convenient, simple, and rapid method for preparation of nano-objects at high concentrations (solids content is typically >10 wt % and ≤ 40 wt %) under relatively non-demanding conditions. Morphology diagrams can be constructed for a fixed degree of polymerization of the hydrophilic block, by varying the degree of polymerization of the core-forming block and the solids content (that is, the final di-block copolymer concentration). This approach enables the desired nano-object morphology to be targeted consistently a posteriori.[11] However, morphologies remain difficult to predict because a constant change of the packing parameter is observed as the hydrophobic block grows, combined with decreased plasticization of the core of the formed objects on conversion of the hydrophobic monomer.

Inspired by the pioneering work of Ferguson et al.,[12] we recently performed the whole PISA process in one-pot in water,[13] from growth of the hydrophilic segment to self-assembly of the final amphiphilic block copolymers. The polymerization of various hydrophilic monomers in water was performed using the reversible addition–fragmentation chain transfer (RAFT) process.[14] The resulting water-soluble macroRAFT agents were subsequently chain extended with a hydrophobic monomer under emulsion polymerization conditions. Control of morphology was achieved by altering the molar mass of the hydrophobic block, or adjusting the pH.[15] Unexpectedly, some PISA systems (prepared in "one-pot" or by sequential steps) invariably led to spherical morphologies, irrespective of the degree of polymerization of the hydrophobic block.[16]

We recently turned our attention to the effect of hydrophile on the PISA process. Targeting alginate-decorated polystyrene spherical nanoparticles, we introduced one to two units of alginate macromonomer into poly(*N*-acryloylmorpholine) (PNAM) to serve as a hydrophilic macroRAFT agent for styrene emulsion polymerization.[16d] Depending on the nature of the alginate (mannuronan or guluronan), its polymerization degree and its localization in the PNAM backbone, drastic changes in the final particle morphologies were observed. The origin of this phenomenon is not fully understood but may be explained by the present work.

Herein, we provide new insight into the PISA process by precisely controlling the position of oligomeric side-chains within the hydrophilic macroRAFT agent. This original approach allows alteration of the size and shape of the hydrophilic block, and consequently of the packing parameter, affording an easy tool to probe the impact of the hydrophilic block architecture on the formation of specific morphologies in PISA. We synthesized four hydrophilic macroRAFT agents, each with a degree of polymerization (DP) of 26. The first was a homopolymer of NAM, denoted $PNAM_{26}$. The three others were copolymers containing 23 units of NAM on average and three units of PEGA ($M_n = 454\ g\,mol^{-1}$). The three copolymers differed only in the position of PEGA units, which were introduced either exclusively at the beginning ($P(NAM_8\text{-}co\text{-}PEGA_3)\text{-}b\text{-}PNAM_{15}$), or statistically along the entirety ($P(NAM_{23}\text{-}co\text{-}PEGA_3)$), or exclusively at the end ($PNAM_{15}\text{-}b\text{-}P(NAM_8\text{-}co\text{-}PEGA_3)$) of the copolymer chains (Scheme 1; Supporting Information, Table S1). NAM and PEGA comonomers were chosen because they exhibit similar hydrophilic character, no sensitivity to pH value, and no intermolecular hydrogen bonding (both are hydrogen bond donors, water being the only acceptor in our system).

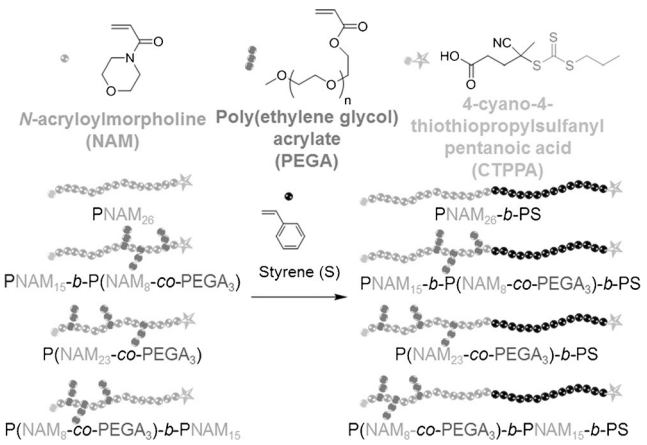

Scheme 1. Chemical structures of monomers, 4-cyano-4-thiothiopropylsulfanylpentanoic acid (CTPPA) control agent, and the structure of the hydrophilic macroRAFT architectures with their corresponding amphiphilic block copolymers.

The impact of these differing macroRAFT agent structures on the final particle morphology was compared for styrene polymerization in water, targeting the same molar mass for the polystyrene block. Our previous work[16d] has shown that spheres are systemically produced for polystyrene polymerization degrees between 150 and 1200 when using $PNAM_{26}$. Nevertheless, a lower DP (90) was chosen in this work to accentuate the impact of a small number of introduced PEGA units. Additionally, none of the macroRAFT agents synthesized for this study show a lower critical solution temperature (LCST) at the emulsion polymerization temperature (80 °C). Any morphological changes can therefore be related to differences in the hydrophilic block architecture. $PNAM_{26}$ was first synthesized by RAFT polymerization in water (Supporting Information, Figures S1–S3) and then directly used for styrene polymerization. $PNAM_{26}$-mediated PISA was very well-controlled, as shown by a shift towards high molar masses and the low dispersities ($Đ$) obtained for the final latex (Figure 1 A; Supporting Information, Table S2). As reported in our previous studies,[16d] monodisperse and spherical particles (Figure 2 A) were obtained with a diameter ($D_n = 30.3$ nm, $D_w/D_n = 1.07$) consistent with particles composed of self-assembled PNAM-*b*-PS block copolymers. Transmission electron microscopy (TEM) observations were corroborated by small-angle X-ray scattering (SAXS) analyses (Figure 3). Scattering intensities were well fitted using a spherical form factor, giving a diameter of 38 nm ($\sigma = 0.15$).

$PNAM_{15}\text{-}b\text{-}P(NAM_8\text{-}co\text{-}PEGA_3)$ was obtained by first polymerizing 15 units of NAM in water using RAFT. In a second step, the resulting $PNAM_{15}$ macroRAFT was successfully extended with a mixture of NAM and PEGA (molar ratio 8/3; Supporting Information, Figures S6 and S7). Individual conversions of NAM and PEGA were similar

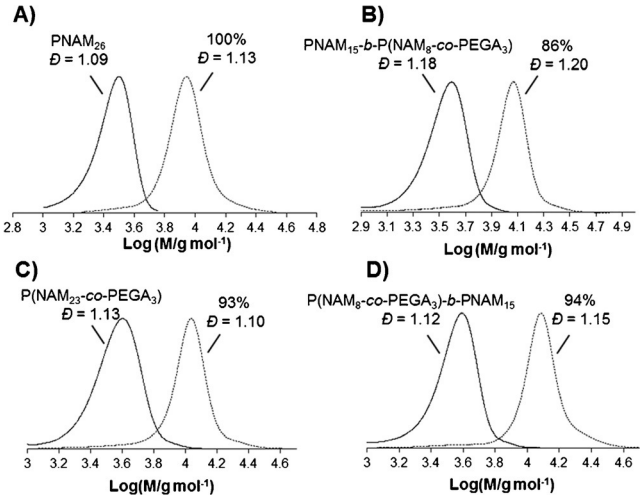

Figure 1. SEC chromatograms of the macroRAFT architectures and of the final polymers after styrene emulsion polymerization mediated by A) $PNAM_{26}$, B) $PNAM_{15}$-*b*-$P(NAM_8$-*co*-$PEGA_3)$, C) $P(NAM_{23}$-*co*-$PEGA_3)$, and D) $P(NAM_8$-*co*-$PEGA_3)$-*b*-$PNAM_{15}$.

(Supporting Information, Figure S5), showing that the two monomers were statistically copolymerized during the second step leading to the targeted structure.

Styrene polymerization mediated by $PNAM_{15}$-*b*-$P(NAM_8$-*co*-$PEGA_3)$ macroRAFT led to well-controlled $PNAM_{15}$-*b*-$P(NAM_8$-*co*-$PEGA_3)$-*b*-PS amphiphilic block copolymers, as attested by a shift toward high molar mass and a low $Đ$ observed after size-exclusion chromatography (SEC) analyses (Figure 1B; Supporting Information, Table S2). Rather than obtaining small spheres, large vesicles were the predominant morpholology (Figure 2B), in conjunction with a very minor population of fibers (Supporting Information, Figure S8). SAXS intensities displayed in Figure 3 showed the form factor characteristic of unilamellar vesicles and did not show the presence of rod-like morphology (which would have given a q^{-1} power law in the high q-range). This suggests that the objects obtained here were in fact primarily vesicles and the observed fibers were indeed present in a relatively small amount. Introduction of three PEGA units, located close to the interface between the hydrophobic and the hydrophilic blocks, was thus enough to perturb the PISA system that was systematically giving rise to spherical morphologies with $PNAM_{26}$. The sole presence of PEGA units in the hydrophilic block definitely has an impact on morphology, and may locally rigidify the hydrophilic backbone and strongly lower the curvature obtained when pure PNAM is employed.

To confirm whether the effect described above was related to specific localization of the PEGA units in the hydrophilic segment, $P(NAM_{23}$-*co*-$PEGA_3)$ macroRAFT was further investigated for the polymerization of styrene. Copolymerization of NAM and PEGA generated a well-defined statistical copolymer with similar consumption of the two monomers (Supporting Information, Figures S9–S11). Styrene polymerization mediated by this macroRAFT was very well controlled (Figure 1C; Supporting Information,

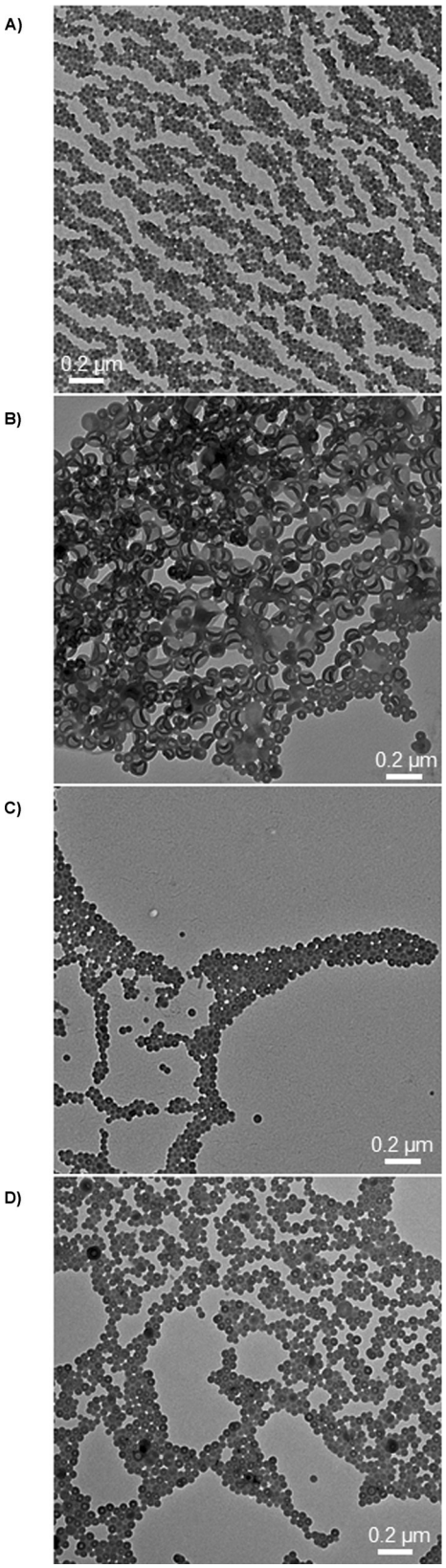

Figure 2. TEM images of the final nano-objects obtained after styrene emulsion polymerization mediated by A) $PNAM_{26}$, B) $PNAM_{15}$-*b*-$P(NAM_8$-*co*-$PEGA_3)$, C) $P(NAM_{23}$-*co*-$PEGA_3)$, and D) $P(NAM_8$-*co*-$PEGA_3)$-*b*-$PNAM_{15}$.

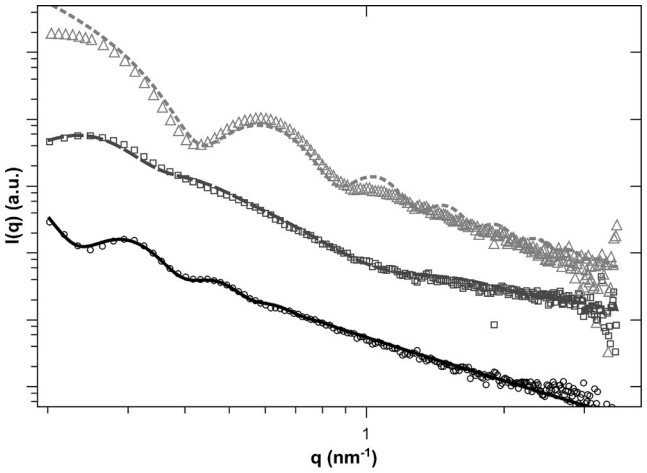

Figure 3. Analysis of the final polymer dispersions ($DP_{PS} = 90$) by synchrotron-based SAXS; that is, measured scattering intensity $I(q)$ as a function of the magnitude of the scattering vector q. Plots are experimental data from $PNAM_{26}$-*b*-PS (——○——), P(NAM_{23}-*co*-$PEGA_3$)-*b*-PS (– – –□– – –), $PNAM_{15}$-*b*-P(NAM_8-*co*-$PEGA_3$)-*b*-PS (-----△-----). Solid curves represent modeling of the SAXS data, assuming a dispersion of non-interacting polydisperse objects ($S(q) = 1$), using the form factors of a sphere (○ $r = 18$ nm), and of unilamellar vesicles (□ $r = 14$ nm, $t = 5$ nm; △ $r = 70$ nm, $t = 14.5$ nm).

Table S2). However, the resulting P(NAM_{23}-*co*-$PEGA_3$)-*b*-PS amphiphilic block copolymers self-assembled into a mixture of nanometric vesicles and small spheres (the average size of nano-objects was $D_n = 36.0$ nm, $D_w/D_n = 1.08$; Figure 2C). TEM images also show a very minor population of tubular structures[4a] (Supporting Information, Figure S12).

Further structural information was obtained by SAXS analyses (Figure 3). The SAXS trace does not show an obvious cylindrical form factor but rather a lamellar dominated form factor. Solution assemblies contained a majority of vesicles, as well as a very small amount of cylinders. The SAXS trace cannot be fitted perfectly by a vesicle form factor because scatterers with other shapes are present. Indeed, scattering intensities were in good agreement with vesicle structures having an inside diameter of 14 nm and a polymer layer thickness (t) of 5 nm, showing that the main morphologies are likely nanovesicles. A q^{-1} power law is observed at high q range, which is consistent with the presence of rod-like objects, as shown in the TEM observations. The different morphologies obtained with this macroRAFT architecture confirmed that the proximity of the PEGA units to the hydrophobe–water interface is responsible for the formation of the large vesicles obtained with $PNAM_{15}$-*b*-P(NAM_8-*co*-$PEGA_3$) macroRAFT.

When P(NAM_8-*co*-$PEGA_3$)-*b*-$PNAM_{15}$ (see synthesis; Supporting Information, Figures S13-S15) was used as a macroRAFT, morphologies similar to those obtained with P(NAM_{23}-*co*-$PEGA_3$) were obtained (Figure 2D; Supporting Information, Table S2). A mixture of nanometric vesicles and spheres (average size: $D_n = 42.8$ nm, $D_w/D_n = 1.04$) and a very small amount of "double-walled fibers"[4a] (Supporting Information, Figure S16) was generated. Control of polymerization and formation of amphiphilic block copolymers remained as good as that described in the previous experiments (Figure 1D). In P(NAM_8-*co*-$PEGA_3$)-*b*-$PNAM_{15}$ there are no opportunities for a PEGA unit to be close to the PS segment, while in P(NAM_{23}-*co*-$PEGA_3$) the probability is very low. In both of these cases the hydrophilic block segment close to the interface is not rigidified and the packing parameter is intermediate between that of the pure PNAM system and the system with side-chain PEGA units close to the interface ($PNAM_{15}$-*b*-P(NAM_8-*co*-$PEGA_3$)). Mixed morphologies between spheres and vesicles are therefore favored.

To gain further understanding of the morphology changes, a preliminary molecular dynamic simulation was performed (provided in the Supporting Information). $PNAM_{15}$-*b*-P(NAM_8-*co*-$PEGA_3$) and P(NAM_{23}-*co*-$PEGA_3$)-based systems (with side-chains potentially lying close to the hydrophobic block) led to objects with a smaller aggregation number than PNAM or P(NAM_8-*co*-$PEGA_3$)-*b*-$PNAM_{15}$ systems (lacking side-chains, or located far from the hydrophobic block; Supporting Information, Figure S17). The simulation suggests that the presence of side-chains impacts on the dynamics of the self-assembly process. Therefore, the drastic change of morphology obtained with $PNAM_{15}$-*b*-P(NAM_8-*co*-$PEGA_3$) (formation of large vesicles) might be the result of geometric constraints (packing parameter) as well as of a modification of self-assembly kinetics.

In conclusion, we have shown that introduction of only three PEGA units to the hydrophilic segment of amphiphilic block copolymers, obtained by PISA, impacted strongly on the final morphology. The presence of PEGA close to the PS hydrophobic segment achieved vesicle morphology that could not be obtained with a pure PNAM system, whatever the molar mass of the hydrophobic block. The controlled radical polymerization technique involved in PISA, namely the RAFT process described herein, was advantageously used to architect a hydrophilic segment, and will contribute to a greater understanding of the self-assembly that occurs during polymerization. This tool holds great promise in the formation of pure morphologies.

Acknowledgements

The authors warmly thank Dr. Samuel Pearson and Nesrine Mansouri (C_2P_2) for very fruitful discussions.

Keywords: amphiphiles · nanoparticles · RAFT polymerization · self-assembly · water

How to cite: *Angew. Chem. Int. Ed.* **2016**, *55*, 3739–3743
Angew. Chem. **2016**, *128*, 3803–3807

[1] I. Hamley, *Block Copolymers in Solution: Fundamentals and Applications*, Wiley, Hoboken, **2005**.
[2] a) Y. Mai, A. Eisenberg, *Chem. Soc. Rev.* **2012**, *41*, 5969–5985; b) R. C. Hayward, D. J. Pochan, *Macromolecules* **2010**, *43*, 3577–3584.
[3] a) L. Zhang, A. Eisenberg, *Science* **1995**, *268*, 1728–1731; b) N. S. Cameron, M. K. Corbierre, A. Eisenberg, *Can. J. Chem.* **1999**, *77*, 1311–1326.

[4] a) M. Antonietti, S. Förster, *Adv. Mater.* **2003**, *15*, 1323 – 1333; b) A. Blanazs, S. P. Armes, A. J. Ryan, *Macromol. Rapid Commun.* **2009**, *30*, 267 – 277.
[5] J. Israelachvili, *Intermolecular and Surface Forces*, *3rd ed.*, Academic Press, London, **2011**.
[6] J. C. M. van Hest, D. A. P. Delnoye, M. W. P. L. Baars, M. H. P. van Genderen, E. W. Meijer, *Science* **1995**, *268*, 1592 – 1595.
[7] M.-P. Chien, A. M. Rush, M. P. Thompson, N. C. Gianneschi, *Angew. Chem. Int. Ed.* **2010**, *49*, 5076 – 5080; *Angew. Chem.* **2010**, *122*, 5202 – 5206.
[8] A. P. Martinez, Z. Cui, C. Hire, T. A. P. Seery, D. H. Adamson, *Macromolecules* **2015**, *48*, 4250 – 4255.
[9] J. R. Lovett, N. J. Warren, L. P. D. Ratcliffe, M. K. Kocik, S. P. Armes, *Angew. Chem. Int. Ed.* **2015**, *54*, 1279 – 1283; *Angew. Chem.* **2015**, *127*, 1295 – 1299.
[10] a) M. Lansalot, J. Rieger, F. D'Agosto in *Macromolecular self-assembly* (Eds.: O. Borisov, L. Billon), **2016**, in press; b) P. B. Zetterlund, S. C. Thickett, S. Perrier, E. Bourgeat-Lami, M. Lansalot, *Chem. Rev.* **2015**, *115*, 9745 – 9800; c) B. Charleux, G. Delaittre, J. Rieger, F. D'Agosto, *Macromolecules* **2012**, *45*, 6753 – 6765.
[11] N. J. Warren, S. P. Armes, *J. Am. Chem. Soc.* **2014**, *136*, 10174 – 10185.
[12] a) C. J. Ferguson, R. J. Hughes, B. T. T. Pham, B. S. Hawkett, R. G. Gilbert, A. K. Serelis, C. H. Such, *Macromolecules* **2002**, *35*, 9243 – 9245; b) C. J. Ferguson, R. J. Hughes, D. Nguyen, B. T. T. Pham, R. G. Gilbert, A. K. Serelis, C. H. Such, B. S. Hawkett, *Macromolecules* **2005**, *38*, 2191 – 2204.
[13] I. Chaduc, W. Zhang, J. Rieger, M. Lansalot, F. D'Agosto, B. Charleux, *Macromol. Rapid Commun.* **2011**, *32*, 1270 – 1276.
[14] a) C. Barner-Kowollik, *Handbook of RAFT Polymerization*, Wiley-VCH, Weinheim, **2008**; b) D. J. Keddie, G. Moad, E. Rizzardo, S. H. Thang, *Macromolecules* **2012**, *45*, 5321 – 5342; c) D. J. Keddie, *Chem. Soc. Rev.* **2014**, *43*, 496 – 505.
[15] a) W. Zhang, F. D'Agosto, O. Boyron, J. Rieger, B. Charleux, *Macromolecules* **2012**, *45*, 4075 – 4084; b) W. Zhang, F. D'Agosto, P.-Y. Dugas, J. Rieger, B. Charleux, *Polymer* **2013**, *54*, 2011 – 2019.
[16] a) I. Chaduc, M. Girod, R. Antoine, B. Charleux, F. D'Agosto, M. Lansalot, *Macromolecules* **2012**, *45*, 5881 – 5893; b) I. Chaduc, A. Crepet, O. Boyron, B. Charleux, F. D'Agosto, M. Lansalot, *Macromolecules* **2013**, *46*, 6013 – 6023; c) V. J. Cunningham, A. M. Alswieleh, K. L. Thompson, M. Williams, G. J. Leggett, S. P. Armes, O. M. Musa, *Macromolecules* **2014**, *47*, 5613 – 5623; d) I. Chaduc, E. Reynaud, L. Dumas, L. Albertin, F. D'Agosto, M. Lansalot, under revision.

Received: December 2, 2015
Revised: December 30, 2015
Published online: February 15, 2016

